SECED 2023 Conference
Earthquake Engineering & Dynamics for a Sustainable Future
14-15 September 2023, Cambridge, UK

ANALYSING RECORDINGS FROM THE UK'S FIRST BOREHOLE SEISMOMETER ARRAY TO AID MODEL DEVELOPMENT FOR A PSHA AT BRADWELL B

Sarah TALLETT-WILLIAMS[1], Iain TROMANS[2], Guillermo ALDAMA BUSTOS[2], Olga-Joan KTENIDOU[3], Angeliki LESSI-CHEIMARIOU[2] & Fleur STRASSER[2]

Abstract: *The UK's first three-instrument downhole seismometer array was installed at the Bradwell B (BRB) site in Essex, UK, as part of plans to construct a new nuclear power station at the site. The array was designed to provide earthquake records to support a site-specific probabilistic seismic hazard analysis (PSHA). Weak-motion records were collected from 64 earthquakes over an 18-month period covering a distance range of 65 to 520 km and a moment magnitude range of 1.5 to 4.8. Records with sufficient energy based on signal-to-noise ratios were processed to determine transfer functions (TFs) between the near-surface target horizon and the reference velocity horizon (i.e., bedrock); the horizontal/vertical Fourier spectral ratios (HVSR); and vertical/horizontal (V/H) response spectral ratios at the depth of each instrument. Comparisons with elements of the PSHA aided model development and improved confidence in the approach adopted. This paper presents the strategy for selecting the array location, the approach adopted for processing and analysis of the weak-motion records and how these records were used for the verification of aspects of the PSHA model.*

Introduction

Even in areas of low seismicity such as the UK, safety critical facilities are required to be designed to resist seismic loads. Determining the appropriate level of seismic actions for these facilities is essential to establish construction viability for the owners, as well as sufficient safety tolerances for the wider society, who would be adversely impacted by a design failure. Particularly in areas of low seismic hazard, the estimation of the hazard at long return periods is significantly influenced by the large uncertainties associated with the prediction of future earthquakes and the determination of ground motions caused by given earthquakes at the site of interest.

Modern practice in seismic hazard evaluation emphasises the importance of understanding and characterising the uncertainties associated with input parameters and models for probabilistic seismic hazard analysis (PSHA) and site response analysis (SRA). This is highlighted in guidelines from the IAEA (2022) and the ONR (2018).

For major infrastructure projects such as nuclear power stations, targeted up-front investment in technology may help to reduce these uncertainties, for example, the installation of downhole site instrumentation (DSI). This can yield significant benefits in the downstream design and construction, with the potential for increasing confidence at long return periods and providing a basis for the substantiation of the Design Basis Earthquake.

Based on a review of international IAEA safety standards (e.g. IAEA 2021; 2022), ANSI standards (2020) and national recommendations provided by the ONR in the latest TAG 13 (ONR 2018), although not strictly required to fulfil the safety case of a new or existing nuclear facility, the installation of DSI is considered relevant good practice for short and long-term seismic monitoring at nuclear facilities. Additionally, the installation of a DSI meets the requirement to monitor free-field motions as part of the structural monitoring during plant operations as well as an earthquake alerting and shutdown triggering system as recommended by the IAEA safety guides (e.g., IAEA 2021).

The benefits of DSIs to the PSHA for the site evaluation (and future updates as part of the periodic safety review) are three-fold:

[1] Dr, Jacobs, London, UK, sarah.tallettwilliams@jacobs.com
[2] Dr, Jacobs, London, UK
[3] Dr, National Observatory of Athens, Greece

- Estimation of the high-frequency (>5-10 Hz) spectral decay parameter kappa (κ, Anderson and Hough 1984), and associated uncertainty, which enables the adjustment of foreign Ground Motion Prediction Equations (GMPEs) to more site-specific conditions (Ktendiou et al. 2023);
- Calibration of the site response model by comparing numerical transfer functions (TFs) and horizontal-to-vertical Fourier spectral ratios (HVSRs, Lermo and Chavez-Garcia 1994) against empirical data computed from weak-motion records allowing estimation of the uncertainties associated with the numerical modelling; and
- Computation of empirical vertical to horizontal response spectral ratios (V/Hs) that contributed to the development of the V/H model used to compute the vertical response spectra.

The derivation of the κ parameter using data from the DSI at the BRB site (first bullet point above) is discussed in detail in the companion paper by Ktenidou et al. (2023). In this paper, the siting and design of the DSI is described as well as the data recorded. The processing of this data to allow validation of aspects of the PSHA models is outlined. In addition, the preliminary results of this validation are shown and conclusions given about the usefulness of the array to the PSHA study.

Siting and design of the downhole site instrumentation

The DSI was installed in an existing plastic-lined borehole from the PSHA ground investigation campaign which was characterised in terms of dynamic parameters including in situ VS measurements and laboratory testing. The DSI is located within the footprint of the main BRB development area, but away from areas likely to be exposed to persistent ambient ground noise. This was including noise from the adjacent Bradwell A site which, whilst no longer operational, is currently undergoing decommissioning.

The BRB site was subject to an extensive ground investigation including laboratory and field testing for the characterization of the dynamic soil properties. The geology is formed of a series of sub-horizontal layers. These are well known in the London Basin and include the London Clay, Harwich Formation, Woolwich & Reading Beds, Upnor and Thanet Formation with a bedrock of Chalk as described in Figure 1. The soil column is in general soft with shear wave velocity (VS) values ranging from about 200 m/s at the top of the London Clay to around 500 m/s at the base of the Thanet Beds. The top of Chalk represents a significant velocity contrast, having a best-estimate VS of 1,000 m/s.

The DSI installed at the BRB site comprises three Güralp Radian digital broadband seismometers, each with an integral micro electromechanical system (MEMS) accelerometer (with an additional MEMS accelerometer at the surface). It is understood that this was the first multi-instrument broadband DSI installed and operating in the UK. The BRB instruments were specified to have an acceleration response flat over the 0.083-200 Hz interval to provide improved detectability at high frequencies, important for derivation of κ and more appropriate for low-seismicity engineering seismological application. An alternative version of the system settings, with a flat velocity response over the same interval, giving better detectability at low frequencies was considered less relevant for the current application. All instruments were set to sample at 250 Hz to allow for potentially usable records up to 75 Hz. The BRB array is powered by solar panels and it is currently integrated into the UK seismic monitoring network, with data being collected continuously by the British Geological Survey (BGS, e.g. Galloway 2021).

The three broadband triaxial instruments were installed at depths of 10.5 m, 41.7 m and 92.0 m, each instrument targeting a specific geological unit (Figure 1). The deepest sensor (instrument 00) is situated just below the top of the Chalk which was the reference velocity horizon assumed for the PSHA (i.e., bedrock). The embedment depth into the Chalk of the deepest sensor is about 3 m to avoid a thin weathered zone encountered at the top of this unit. The second sensor (instrument 01) was installed between the surface and bedrock instruments to provide records from the base of the London Clay Formation, the founding layer for the nuclear island. The sensor

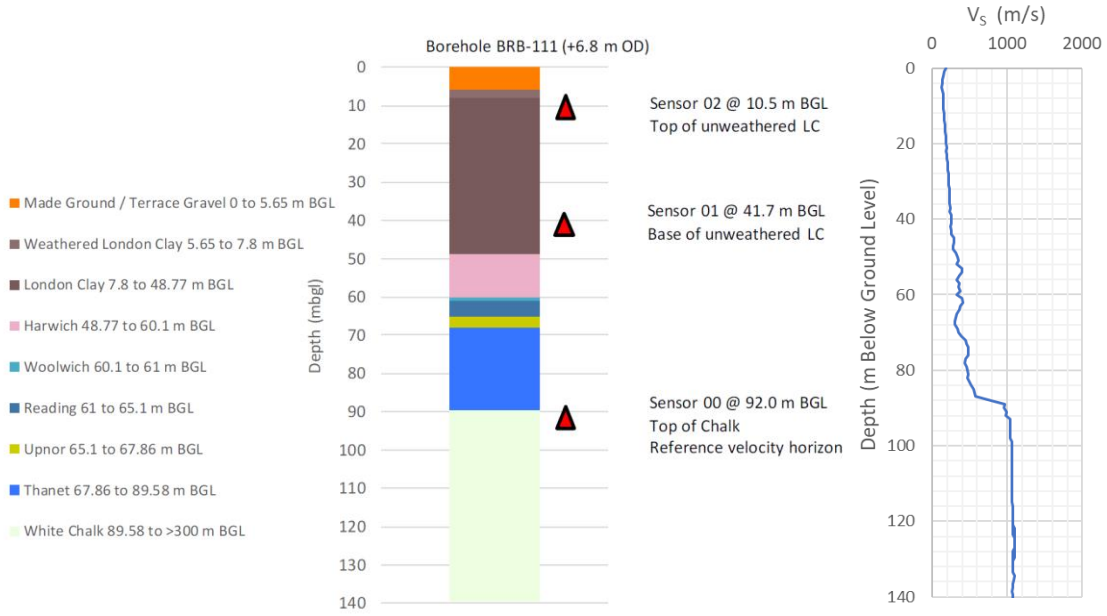

Figure 1. Summary of sensor depths and geological conditions for the BRB DSI (left) and the associated shear wave velocity profile (right).

was installed at the base of this formation providing comparison with the shallowest sensor 02 at the top of the layer. Thus, the effect of this layer on the site response could be isolated, being relatively homogenous compared to the Woolwich & Reading Beds underneath. The top sensor (instrument 02) was situated at the top of the unweathered London Clay Formation, representing the nominal reactor foundation level and the target horizon for the SRA.

One of the main benefits of a downhole array is the inclusion of sensors at various depths to capture the difference in ground motions between the bedrock and the near-surface layers. However, it needs to be considered that ground-motion records from borehole instruments can be affected by destructive interference between up-going waves direct from the earthquake source and down-going waves reflected from the ground surface. Thus, a high-level assessment of the destructive interference effect was performed.

The destructive frequency, f_{dest} is controlled by the depth of the sensor and the average shear-wave velocity V_{S_avg} between the sensor and the surface as given by the relationship (Cadet et al. 2012):

$$f_{dest} = \frac{V_{s\_avg}}{4H} \quad (1)$$

where H is the depth at which the sensor is deployed. From work done by Cadet et al. (2012), Fourier spectral amplitudes in the frequency range between f_{dest} and $5*f_{dest}$ are most affected by destructive interference. If possible, the sensor installation depth should be selected to ensure minimal interaction between the destructive interference frequency range and the high frequency portion of the signal (~above 10 Hz) used to calculate κ. As previously discussed, the location of the sensors was driven by the geology and the interest in knowing the ground motion at specific depths, but cognisance of the destructive interference was considered during the interpretation of the data.

Data collected

The BRB downhole array has been operational since November 2018. The process for the identification and initial processing of the ground-motion records, focusing primarily on the estimation of the parameter κ [see companion paper Ktenidou et al. (2023)], consisted of:

- An initial identification of events at epicentral distances (R_{EPI}) within 500 km from the site, guided by events reported in the monthly BGS Bulletin and by other European agencies (e.g., the European-Mediterranean Seismological Centre; EMSC 2022), as well as records

from the Royal Observatory of Belgium (ROB 2020). The choice of the 500 km radius was guided by the limited number of events within the first 200 km, which would have been the preferred choice.

- Extracting the ground-motion records from the continuous recordings and correcting these for instrument response;
- Picking of the P-wave and S-wave arrival times and selection of the S-wave window for each record; and
- A categorisation of the records based on the usable frequency range from visual inspection of the Fourier amplitude spectra (FAS), for the noise and S-wave windows, and signal-to-noise ratios (SNRs). Although it is common practice to consider only records with SNR ≥ 3, given the limited data from the BRB array a SNR ≥ 1 was considered to define the upper and lower bounds of the usable frequency range.

Following this initial processing, a total of 64 ”usable” events were identified from data recorded between November 2018 and the end of June 2020. For each event three-component (two horizontal and one vertical) ground-motion records for each of the three instruments in the array were provided as summarised in Figure 2. It is noted that the moment magnitudes were derived from local magnitude (ML) determinations using the relationship by Grünthal et al. (2009). The smaller magnitudes are outside the range of applicability of the conversion relationship used, but this was done for consistency with the rest of the catalogue in the study (i.e., the PSHA)

Although the criterion of SNR ≥ 1 may be acceptable for the estimation of κ, using ground-motion records with very low SNR values may have an undesired effect when calculating response spectra and therefore V/H ratios. Thus, each record was classified in terms of SNR (Table 1). Records that had a SNR > 2 within a “reasonable” range of frequencies were classified as ”good”. Records having a SNR > 2 within a ”narrow” frequency range were classified as ”average”. All other records were classified as ”poor”. Note that given the very low intensity of the ground-motion records it was not possible to set a strict definition for a ”reasonable” or ”narrow” range of frequencies. Therefore, a significant amount of expert judgement was used for this classification. As expected, records from the deeper instrument (00) were considerably less noisy than records from the shallower instruments (01 and 02).

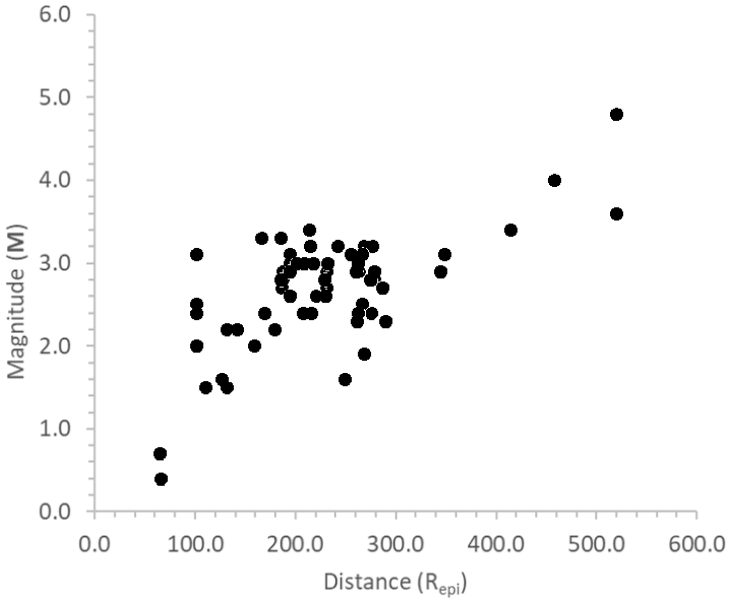

Figure 2. Summary of the BRB dataset in terms of distance and magnitude.

Instrument	Good	Average	Poor
02	10	28	26
01	16	25	23
00	18	34	12

Table 1. Number of records associated with each BRB sensor classified by SNR

Data Processing

Those records classified as “good” or “average” were then processed for calculations. Firstly, we selected a window between 20 s before the arrival of the P-wave and 100 s after the end of the S-wave window. The cut and tapered records were filtered using a Butterworth filter between 0.1 and 100 Hz. To ensure that the cutting and filtering did not negatively affect the characteristics of the records, the data processing procedure described by Akkar et al. (2010) was implemented, which follows the same principles as the NGA-West2 data processing (Kishida et al. 2016). This included Konno and Ohmachi (1998) smoothing which was applied to the calculated Fourier Amplitude Spectra (FAS).

Figure 3 shows the time histories (THs) and SNRs for the east component of the top (02) and base (00) instruments for the **M** 3.1 Newdigate event that occurred on 27 February 2019 recorded at 102 km from the site. The coloured lines on the figure show the used P-wave arrival time, S-wave window and the truncation times of the record. The entire record between the truncated lines was used in the calculations. As part of the QA process, the acceleration, velocity and displacement time-histories for each record were plotted to verify that no residual displacements, filter transients or wrap-around effects were produced as part of the post-processing of the ground-motion records.

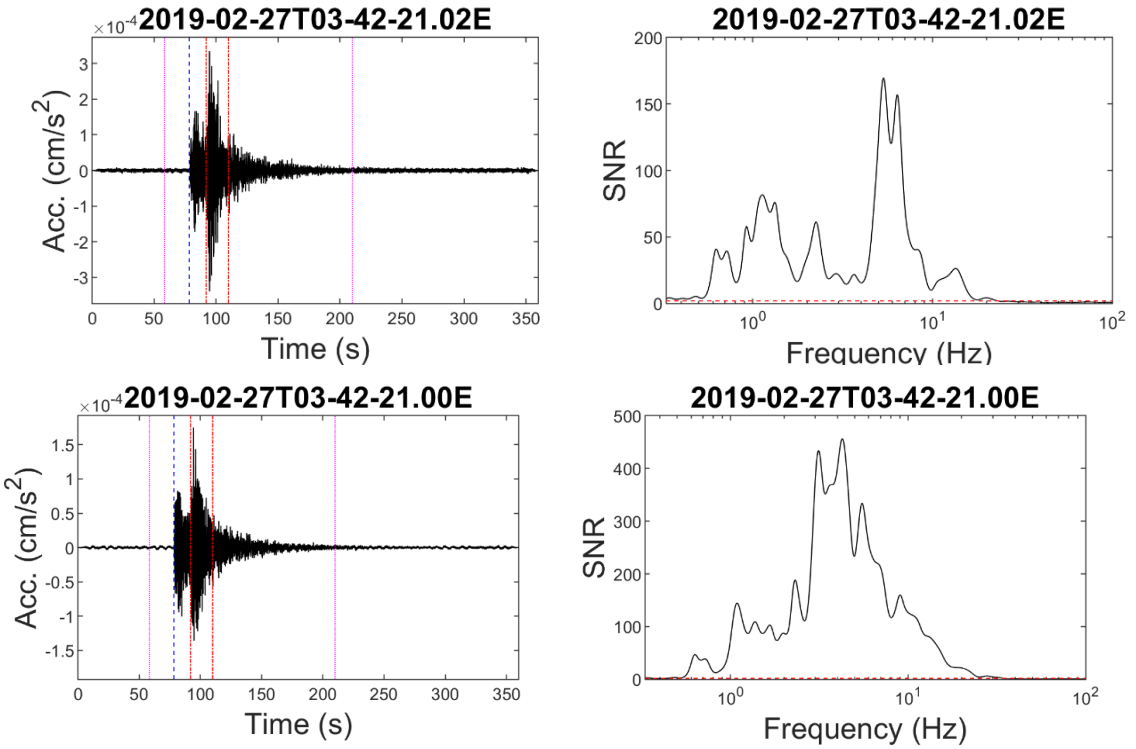

Figure 3. Acceleration time histories for the instrument 02 (10.5 m depth) and instrument 00 (92 m depth; left column) and their corresponding SNRs (right column) for the 2019-02-27 event. In the time histories, the blue dashed line is the used P-wave arrival time and the red are the S-window. The purple lines show the length of the record considered after truncation.

For the calculation of both the TFs (used in the site response calibration) and the V/H ratios (to be used in the development of the V/H model), the horizontal ground motion was taken as the geometric mean of the two horizontal components. The use of the vector sum of the two horizontal components was also explored for the calculation of TFs and V/H ratios; however, a very small difference was observed between the two approaches. Therefore, for consistency with the definition of the horizontal component used by most modern GMPEs and V/H empirical models, the geometric mean approach was retained even though it is not orientation independent.

Empirical Transfer Functions and Horizontal / Vertical Spectral Ratios

Figure 4 shows the mean TFs between instruments 02 (10.5 m depth) and 00 (92 m depth) for the horizontal component, plotted against the 1D linear time series site response model. This numerical model was damped using the small shear strain damping determined from the resonant column tests which were performed in the recent site-specific laboratory campaign. The close alignment of the numerical TFs with the empirical TFs from the recordings of the DSI supported the use of 1D SRA and aided the calibration of the velocity model for SRA.

Figure 5 shows the HVSR from weak-motion records for the shallower instrument (02) and HVSR obtained from microtremor measurements during the ground investigation at the ground surface at the location of the BRB DSI using a Güralp CMG-6TD broadband seismometer. As expected, HVSR from the weak-motion records from the shallowest borehole instrument 02 and the surface microtremor HVSR measurements are well correlated, both capturing a peak at around 0.65 Hz associated with a significant impedance contrast at depth (~350 m below ground level) corresponding to the top of the Silurian/Devonian basement.

The HVSR of earthquake records (or “receiver function”) can be used as a proxy for the site response as it has been shown to capture the predominant peak that would have been observed in a TF computed with respect to a reference site, even if the amplitudes of this peak might not be representative (e.g., Lermo and Chavez-Garcia 1993). This depends on the assumption that the vertical is amplified only slightly and at different frequencies to the horizontal. It should be noted that the HVSR represents the site response of the whole unbounded ground column up to the elevation of the instrument whilst a TF represents the ratio of Fourier amplitudes between the elevations of the instruments. HVSR can therefore provide additional insights to help with the validation of the ground model for SRA (Figure 6). Thus, the TFs from the DSI records aided in the calibration of the shallow velocity model (target level to top of chalk) whilst the HVSR from the DSI improved confidence in the deep velocity profile (top of chalk to top of Silurian/Devonian basement).

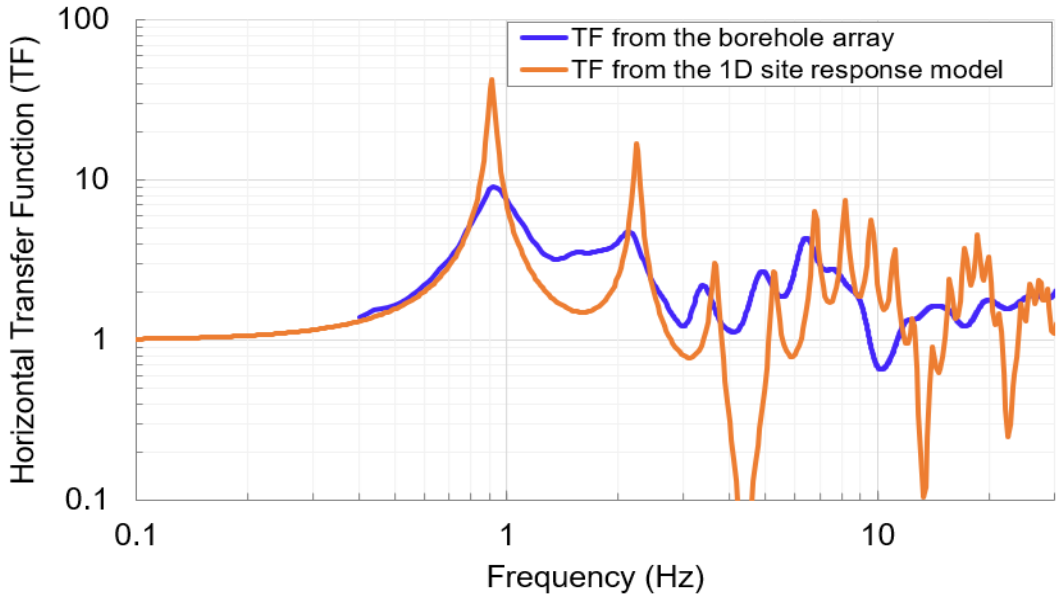

Figure 4. Comparison of the empirical mean TF from the borehole array showing the influence of soil conditions between instruments 02 & 00 with the 1D linear time series TF from the horizontal site response model.

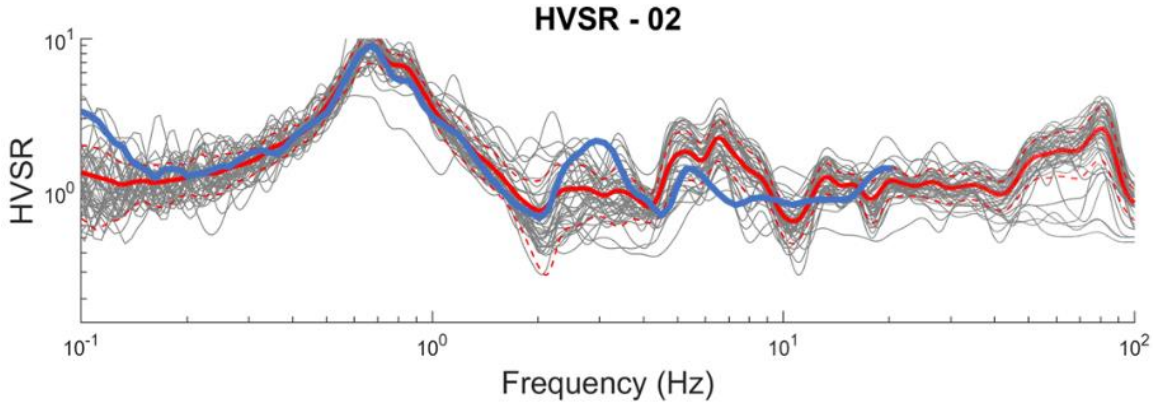

Figure 5. HVSR from all weak-motion records (grey lines) from instrument 02 in the BRB array, mean HVSR (solid red line) +/- 1 standard deviation (dashed red lines) and HVSR from microtremor measurements at the ground surface (solid blue line).

V/H spectral ratios from the BRB array

To determine the vertical motion at the BRB site, the use of the vertical to horizontal (V/H) spectral ratios was adopted. After a thorough review of candidate empirical V/H models, four were chosen for further consideration and comparison with the instrumental data:

- Akkar et al. (2014a;b) [AETAL14];
- Bozorgnia and Campbell (2016a) [BETAL16];
- Gülerce and Abrahamson (2011) [GA11]; and
- Stewart et al. (2016) [SETAL16].

The magnitude and distance ranges in the BRB dataset fall within the range of applicability of all selected empirical models, with the exception of GA11 which is only applicable for magnitudes greater than **M** 5.0. Comparisons between the median predictions from the selected V/H empirical models and the median V/H ratios from the BRB site-specific data are shown in Figure 6 for the base (00) instrument. The site-specific median V/H ratios were calculated as the median of the logarithm of the ratios for each of the records, which is in line with the approach followed by the developers of the empirical V/H models.

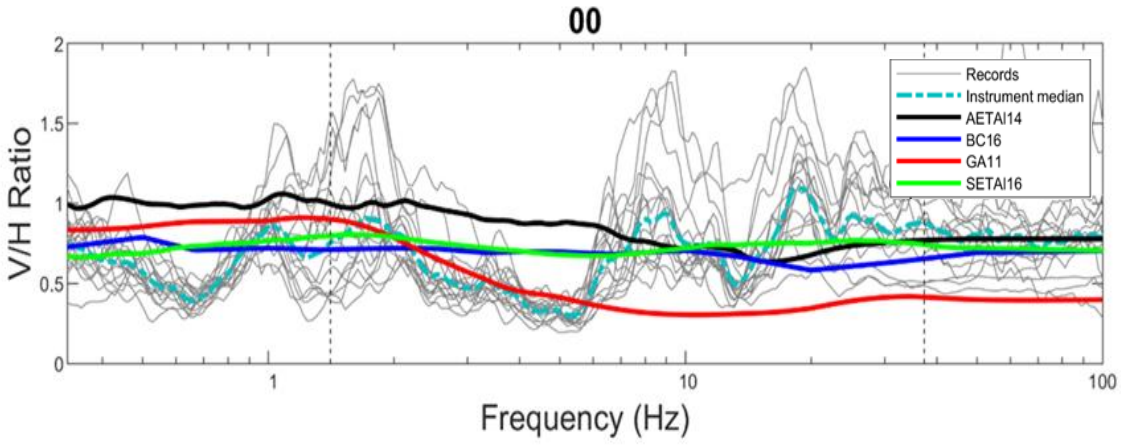

*Figure 6. Comparison of the V/H ratios for the records classified as 'good' for instrument 00 (grey lines) and their median (turquoise dashed line) with the four empirical models selected which were set to **M** 4.0, a distance of 200 km with the relevant V_{S30} for the instrument. Style-of-faulting was set as strike-slip when specifically defined in the empirical model or 'other' for models that only use dummy variables for normal and reverse faults.*

As expected, the V/H ratios from the empirical models are smoother and do not capture the site-specific peaks and troughs seen in the site-specific data. However, the empirical models capture the overall behaviour observed from the data across multiple sites. A good match in terms of the overall V/H value is observed particularly at frequencies above 10 Hz. At frequencies above 2 Hz GA11 consistently predicts lower ratios than the other empirical models and the median from the site-specific data; however, this could be due to the extrapolation of the model to magnitudes lower than its range of applicability. The AETAL14 and SETAL16 models appear to give the best match overall.

An important consideration when comparing predictions from empirical models and the site-specific data is that the V/H ratios from the BRB array are for within motions and likely to be affected by destructive interference whilst the empirical models are based on surface measurements. As the 'within motion' effect from downhole recordings affects only the amplitudes of the response spectra and it is expected to affect by the same amount the vertical and horizontal components for the ground motion, this effect is not expected to be an issue when comparing predictions from empirical models and site-specific data. However, destructive interferences between the upgoing and down going waves could explain some of the peaks and troughs observed in the site-specific data which are not necessarily due to resonance effects.

In addition to comparisons with the predictions of empirical V/H ratios, the low scenario-sensitivity of the (far-field) V/H spectral ratio also enables comparisons of the weak-motion data recorded on the BRB downhole array with V/H spectral ratios from strong-motion data recorded on sites with similar site conditions. Figure 7 shows a comparison between the V/H spectral ratio distribution (median and +/- 1 $\sigma \ln_{VH}$ range) from the shallowest instrument (02) in the BRB downhole array with the V/H spectral ratio distribution of NGA-West2 Californian sites with similar site conditions (V_{S30} from 150 to 240 m/s). As would be expected, the regional NGA-West2 data (Ancheta et al. 2013) have a smoother shape and broader variability than the BRB single-site results, since they are averaged over multiple sites and are likely to have less strong impedance contrasts in the top 30 m. The average amplitudes (excluding site-specific peaks) are broadly consistent in the usable range of the data, with the mismatch at lower frequencies reflecting the limited usable frequency range of the BRB data. It is also interesting to note the consistency of the amplitudes of the higher frequency peak (in the 10-20 Hz) range.

This comparison would indicate that 'non-parametric' V/H spectral ratios calibrated to appropriate site conditions represent a viable alternative to empirical models in terms of providing an ergodic estimate of the V/H spectral ratio distribution.

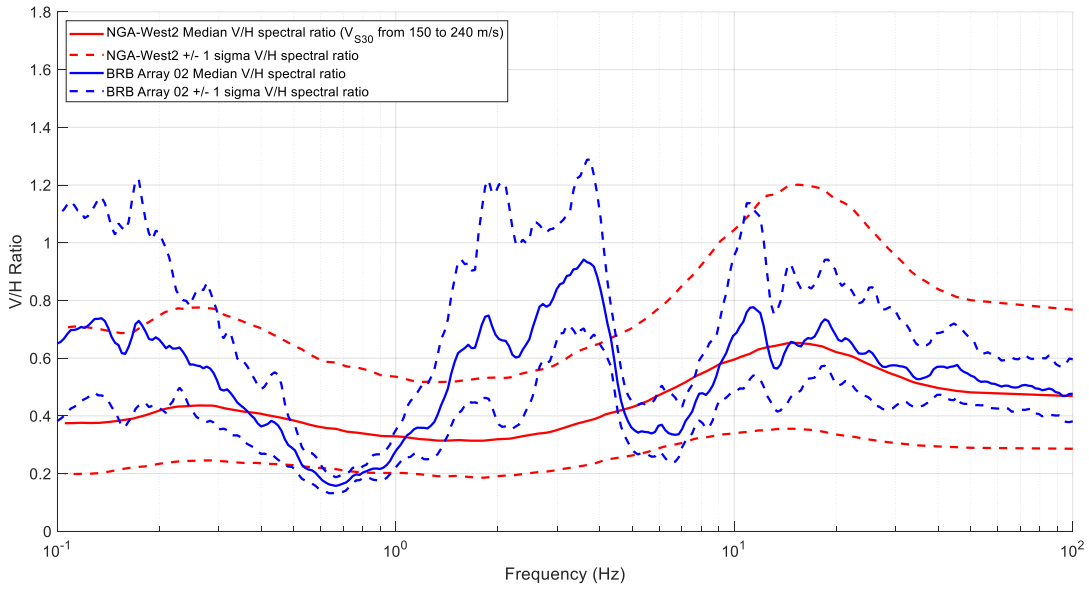

Figure 7. Comparison of V/H spectral ratio distribution from instrument 02 in the BRB downhole array with the V/H spectral ratio distribution of NGA-West2 sites with similar site conditions.

Conclusions

Following collection of approximately 18 months' weak-motion data at BRB, the array records were processed and analysed to help inform development of three elements of the PSHA model:

- Calibration of the site response velocity model (horizontal and vertical), by providing site-specific Fourier transfer functions using pairs of instruments at different levels;
- Association of low frequency peak with a deep impedance contrast (~350 m below ground level); and
- Development of the vertical ground-motion model through calculation of the vertical to horizontal (V/H) response spectral ratio.

For each element of the model, the data helped to better constrain the best estimate and associated uncertainties, contributing to an improved hazard estimate. In spite of the short period of operation of the array in what is a low to very low seismicity region, even by UK standards, a sufficient number of records was obtained to allow a robust assessment of the site response in the linear-elastic range, in both horizontal and vertical directions. This was achieved thanks to high-quality, high-sensitivity instruments, with low sensor noise and the installation of these instruments at depth, which helped to significantly reduce ambient noise. It is hoped with more operating time, further earthquakes will be recorded and the DSI will continue to help improve characterisation of the site-specific ground motions and their uncertainties and ultimately contribute towards the safety of the power plant.

Acknowledgements

The authors would like to thank BRB GenCo for agreeing to the publication of this paper. We are also grateful to the BGS for the collection and provision of the ground-motion records used.

References

Akkar, S., Çağnan, Z., Yenier, E., Erdoğan, Ö., Sandıkkaya, M. A., and Gülkan, P. (2010). The recently compiled Turkish strong motion database: preliminary investigation for seismological parameters. *Journal of Seismology,* 14(3): 457-479.

Akkar, S., Sandıkkaya, M. A., and Ay, B. Ö (2014a). Compatible ground-motion prediction equations for damping scaling factors and vertical-to-horizontal spectral amplitude ratios for the broader Europe region. Bulletin of Earthquake Engineering, 12(1): 517–547.

Akkar, S., Sandıkkaya, M. A., and Ay, B. Ö. (2014b). "Erratum to: Compatible ground-motion prediction equations for damping scaling factors and vertical-to-horizontal spectral amplitude ratios for the broader Europe region." Bulletin of Earthquake Engineering, 12(3): 1429–1430.

Ancheta, T.D., Darragh, R.B., Stewart, J.P., Seyhan, E., Silva, W.J., Chiou, B.S.J., Woodell, K.E., Graves, R.W., Kottke, A.R., Boore, D.M., Kishida, T and Donahue, J.L. (2013). PEER NGA-West2 database. Pacific Earthquake Engineering Research Centre PEER 2013/03

Anderson, J. G. and Hough, S. E. (1984). A model for the shape of the Fourier amplitude spectrum of acceleration at high frequencies. *Bulletin of the Seismological Society of America*, 74 (5): 1969-1993.

ANSI/ANS (2020). *Criteria for investigations of nuclear facility sites for seismic hazard assessments.* American Nuclear Society / American National Standards Institute.

Bozorgnia, Y., and Campbell, K. W. (2016). Ground motion model for the Vertical-to-Horizontal (V/H) ratios of PGA, PGV, and response spectra. *Earthquake Spectra*, 32(2): 951–978.

Cadet, H., Bard, P.-Y., and Rodriguez-Marek, A. (2012). Site effect assessment using KiK-net data: Part 1. A simple correction procedure for surface/downhole spectral ratios. *Bulletin of Earthquake Engineering*, 10(2): 421-448

EMSC (2022). *European-Mediterranean Seismological Centre.* [Online] https://www.emsc-csem.org/#2 (Last accessed 2022/03/11).

Galloway, D.D. (2021). The British Geological Survey Earthquake Bulletin for 2020. BGS Internal Report OR/21/005

Gülerce, Z., and Abrahamson, N. (2011). Site-specific design spectra for vertical ground motion. *Earthquake Spectra*, 27(4): 1023-1047.

Grünthal, G., Wahlström, R., and Stromeyer, D. (2009). The unified catalogue of earthquakes in central, northern, and northwestern Europe (CENEC) - Updated and expanded to the last millennium. *Journal of Seismology,* 13(4), 517-541.

Kishida, T., Ktenidou, O., Darragh, R. B. and Silva, W. J. (2016). Semi-Automated Procedure for Windowing Time Series and Computing Fourier Amplitude Spectra for the NGA-West2 Database, PEER Report 2016-02. Pacific Earthquake Engineering Research Center, University of California, Berkeley, CA.

Konno, K. and Ohmachi, T. (1998). Ground-motion characteristics estimated from spectral ratio between horizontal and vertical components of microtremor. *Bulletin of Seismological Society of America*, 88, 228-241.

Ktendiou, O.J., Pikoulis, E. and Aldama-Bustos G. (2023) Attenuation at the UK's first downhole array. In *SECED 2023: Earthquake Engineering & Dynamics for a Sustainable Future.* Cambridge, 14-15 September.

IAEA (2021). *Seismic design for nuclear installations*. IAEA Safety Standards No. SSG-67 International Atomic Energy Agency, Vienna

IAEA (2022). *Methodologies for seismic soil–structure interaction analysis in the design and assessment of nuclear installations.* IAEA-TECDOC-1990, International Atomic Energy Agency, Vienna

Lermo, J. and Chavez-Garcia, F.J. (1994). Are microtremors useful in site response evaluation? *Bulletin of the Seismological Society of America* 84(5): 1350-1364

ONR (2018). *ONR expert panel on natural hazards. NS-TAST-GD-013 Annex 1 reference paper: Analysis of seismic hazards for nuclear sites.* Expert Panel Paper No: GEN-SH-EP-2016-1, Office for Nuclear Regulation

ROB (2020) *Recent Earthquakes*. http://seismologie.be/en [Accessed June 2020]

Stewart, J. P., Boore, D. M., Seyhan, E., and Atkinson, G. M. (2016). NGA-West2 Equations for Predicting Vertical-Component PGA, PGV, and 5%-Damped PSA from Shallow Crustal Earthquakes. *Earthquake Spectra*, 32(2): 1005–1031.